

Optical Engineering

SPIDigitalLibrary.org/oe

Tetrahedron-based orthogonal simultaneous scan for cone-beam computed tomography

Ivan B. Ye
Ge Wang

Tetrahedron-based orthogonal simultaneous scan for cone-beam computed tomography

Ivan B. Ye^{a,b} and Ge Wang^a

^aVirginia Polytechnic Institute and State University, Blacksburg, Virginia 24061

^bWest High School, Iowa City, Iowa 52241

E-mail: ivan-ye@uiowa.edu

Abstract. In this article, a cone-beam computed tomography scanning mode is designed using four x-ray sources and a spherical sample. The x-ray sources are mounted at the vertices of a regular tetrahedron. On the circumsphere of the tetrahedron, four detection panels are mounted opposite of each vertex. To avoid x-ray interference, the largest half angle of each x-ray cone beam is $27^{\circ}22'$, while the radius of the largest ball fully covered by all the cone beams is 0.460, when the radius of the circumsphere is 1. A proposed scanning scheme consists of two rotations about orthogonal axes, such that, each quarter turn provides sufficient data for theoretically exact and stable reconstruction. This design can be used in biomedical or industrial settings, such as when a sequence of reconstructions of an object is desired. © 2012 Society of Photo-Optical Instrumentation Engineers (SPIE). [DOI: 10.1117/1.OE.51.8.080502]

Subject terms: x-ray; computed tomography; cone-beam computed tomography; computed tomography scanning; tetrahedron; polyhedron; region of reconstruction.

Paper 120667L received May 15, 2012; revised manuscript received Jul. 4, 2012; accepted for publication Jul. 6, 2012; published online Aug. 6, 2012.

1 Introduction

Introduced in 1973, x-ray computed tomography (CT) was a great step for medicine. CT designs with multiple x-ray sources increase temporal resolution, which is an important goal for dynamic imaging applications. Multi-source CT designs so far, however, are mostly based on circular, spiral, or saddle like scanning curves and target a long object, such as a patient or an animal.

While the aforementioned long object problem is important, many existing and emerging applications deal with spherical objects. Pathological samples are often spherical and can be tomographically examined in detail. Industrial parts have irregular shapes, but they are more or less compact and can be fit into a spherical support. Regenerative pharmacology is a new frontier in which engineered tissue or cell culture test beds can be made into multiple clusters for tomographic imaging. In these and other applications, high resolution is an inherent request and takes long data acquisition time due to a limited x-ray photo flux from a micro-focused x-ray focal spot.

To accelerate data acquisition and improve temporal resolution, the multi-source strategy has been used before in cone-beam geometry, as mentioned above. The modern x-ray source

technology, such as carbon nanotube x-ray source techniques, promises a realistic possibility that distributed sources become practical. Thus, employing multiple sources for parallel data acquisition from a spherical object yields an outstanding research opportunity. Theoretically exact, stable, and ultrahigh resolution cone-beam image reconstruction can be achieved.

We propose a scanning scheme for multi-source reconstruction of a spherical object. Basically, four x-ray sources are mounted at the vertices of a regular tetrahedron and are scanned over its circumsphere as illustrated in Fig. 1. Each x-ray source will project an x-ray cone beam towards the opposite face of the tetrahedron, and a reception or detection panel is mounted on the circumsphere behind each face of the tetrahedron as illustrated in Fig. 2. In this setting, the four x-ray cone beams can work simultaneously, without interference, when the half angle of each cone beam is no more than $27^{\circ}22'$ as computed below in Fig. 3(a). Four of these cone beams will simultaneously cover a ball of radius 0.460 for a unit circumsphere of the tetrahedron, as shown in Fig. 3(b).

2 Scanning Mechanism

The rotation of a sphere is a 3D motion governed by the rotation about the axes through the center of the sphere. Without loss of generality, we will restrict ourselves to the composition of 2D rotations about an x-axis and a z-axis. Technically, we propose mounting the circumsphere on a slip ring, which can be rotated about the x-axis that is the principal axis of the slip ring. Then, the slip ring itself is rotated about the vertical z-axis as shown in Fig. 1. From the perspective of symmetry, we let the four vertices of the tetrahedron have equal magnitudes of rotation about the x-axis, and place the tetrahedron in such a way that all vertices are of equal distances to the x-axis. The resulting loci of the four vertices, from this composite rotation, depend on the ratio of rotation speeds about the x-axis and z-axis and will be studied in the later sections.

In our architectural design, slip ring itself can rotate while the object disk rotates in the opposite direction at the same angular speed, as shown in Fig. 1. More specifically, the gray frames and the central object disk are attached to the slip ring. Thus, the rotation of the slip ring itself about the z-axis will make the gray arms and object disk rotate in the same manner. To offset this rotation, the object disk will rotate in the opposite direction so that the object inside the tetrahedron remains stable. At the same time, the circumsphere rotates through the slip ring. This design is desirable when the object is required to be stable. The radius of the largest object sphere that can fit into these tetrahedral scan is computed to be 0.460 for a unit circumsphere.

3 Orthogonal Rotations of the Tetrahedron

As shown in Fig. 1, the scanning consists of orthogonal rotations about the x-axis and z-axis. Note that the x-axis changes its direction as a result of the rotation about the z-axis. The scanning curves depend on the ratio of the rotation speeds. Let b be the ratio of the rotation speed about the z-axis to the rotation speed about the x-axis. Then the composite motion of the four vertices is given by:

$$\begin{aligned} x &= \frac{\sqrt{3}}{3} \cos bt - \frac{\sqrt{6}}{3} \sin t \sin bt, & y &= \frac{\sqrt{6}}{3} \cos t, \\ z &= \frac{\sqrt{6}}{3} \sin t \cos bt + \frac{\sqrt{3}}{3} \sin bt; \end{aligned} \quad (1)$$

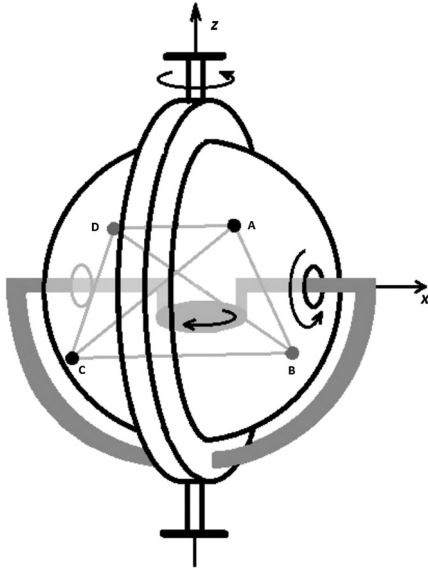


Fig. 1 Orthogonal rotation of a regular tetrahedron with x-ray sources at its four vertices. The gantry and disk are rotated in opposite directions to make the object stable. Vertices A, B, C and D are moving according to Eqs. (1) through (4), respectively.

$$\begin{aligned} x &= \frac{\sqrt{3}}{3} \cos bt + \frac{\sqrt{6}}{3} \sin t \sin bt, & y &= -\frac{\sqrt{6}}{3} \cos t, \\ z &= -\frac{\sqrt{6}}{3} \sin t \cos bt + \frac{\sqrt{3}}{3} \sin bt; \end{aligned} \quad (2)$$

$$\begin{aligned} x &= -\frac{\sqrt{3}}{3} \cos bt - \frac{\sqrt{6}}{3} \cos t \sin bt, & y &= -\frac{\sqrt{6}}{3} \sin t, \\ z &= \frac{\sqrt{6}}{3} \cos t \cos bt - \frac{\sqrt{3}}{3} \sin bt; \end{aligned} \quad (3)$$

$$\begin{aligned} x &= -\frac{\sqrt{3}}{3} \cos bt + \frac{\sqrt{6}}{3} \cos t \sin bt, & y &= \frac{\sqrt{6}}{3} \sin t, \\ z &= -\frac{\sqrt{6}}{3} \cos t \cos bt - \frac{\sqrt{3}}{3} \sin bt. \end{aligned} \quad (4)$$

We will only consider the case of $b = 1$ in this paper. When $b = 1$, the two rotations have the same speed. The resulting composite rotations of the circumsphere and its tetrahedron are illustrated in Figs. 3(b), 4, Video 1, and Video 2 for $b = 1$. In the figure and video, the curve of Eq. (1) is in red, Eq. (2) in green, Eq. (3) in blue, and Eq. (4) in black.

According to theory on cone-beam reconstruction, the region of theoretically exact and stable reconstruction consists of all points through which any plane would contain at least one source point.¹ This is equivalent to the condition that any plane passing through a point to be reconstructed intersects scanning loci at least once almost everywhere, also known as the point-based condition for data completeness for cone-beam scanning. For parallel-beam scanning, a similar data completeness condition was first proved by Orlov in 1975.²

We will also need the concept of an inter-PI-lines.³ When there are multiple x-ray sources, an inter-PI-line is a line

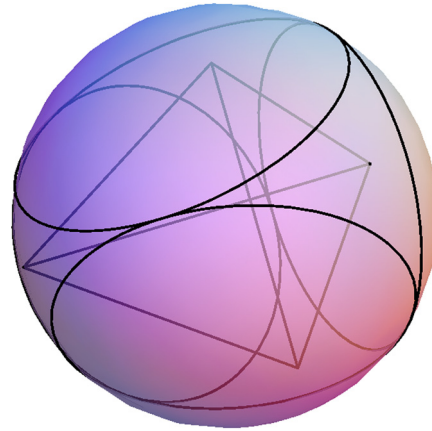


Fig. 2 An x-ray source is mounted on each vertex of the tetrahedron. Four detection panels are mounted on the circumsphere bounded by four lesser circles which are tangent to each other.

segment that has one endpoint on a scanning curve and its other endpoint on another scanning curve. We will find regions of reconstruction by determining all PI-lines, and inter-PI-lines, for the tetrahedral scanning. In particular, we will find all boundary PI-lines, and inter-PI-lines, to determine the boundary surfaces of the reconstruction regions as motivated by Ye et al. in 2009.⁴

In this case, each vertex travels along a large closed curve and a small loop for each period of 2π , as seen in Fig. 3. When $0 \leq t \leq \pi/2$, the paths of three vertices join to form a big closed curve while the other vertex traverses a small loop. The same happens for $\pi/2 \leq t \leq \pi$, $\pi \leq t \leq 3\pi/2$, and $3\pi/2 \leq t \leq 2\pi$, with switching roles of the vertices. This phenomenon is similar to the case when the vertex of the tetrahedron is fixed and other three vertices are rotated by $2\pi/3$, so that the loci of the three vertices form a circle, and then switches vertices and repeats.

Our results suggest the following reconstruction scheme: For $-\pi/2 \leq t \leq \pi/2$, we first reconstruct according to Fig. 5. Then, for $0 \leq t \leq \pi$, we reconstruct a region like Fig. 4, but with a different orientation. After that, we get a new reconstruction for each quarter turn using data from the current and previous quarter turns. When the tetrahedron is rotated continuously, as in Figs. 1, 4 and Video 2, we get four successive reconstructions in each complete cycle of the object contained in the inner sphere in Fig. 2.

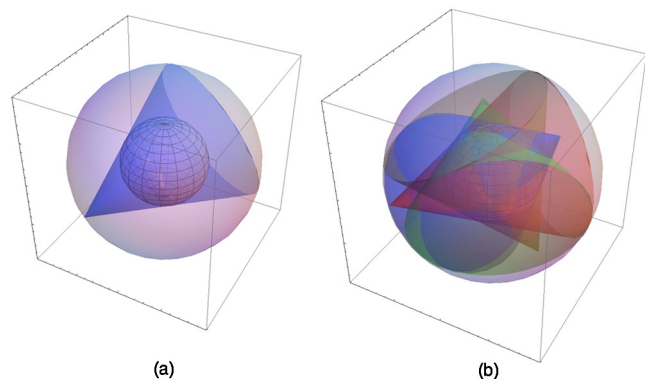


Fig. 3 (a) A cone beam from each tetrahedral vertex contains a concentric ball of radius 0.460. (b) A tetrahedral scanning of four cone beams when $b = 1$ (Video 1, QuickTime, 9.1 MB) [DOI: <http://dx.doi.org/10.1117/1.OE.51.8.080502.1>].

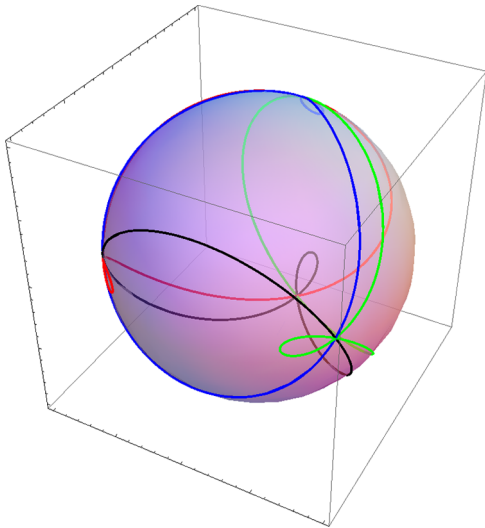


Fig. 4 Scanning paths of vertices of the orthogonally rotating tetrahedron when $b = 1$ (Video 2, QuickTime, 5.22 MB) [DOI: <http://dx.doi.org/10.1117/1.OE.51.8.080502.2>].

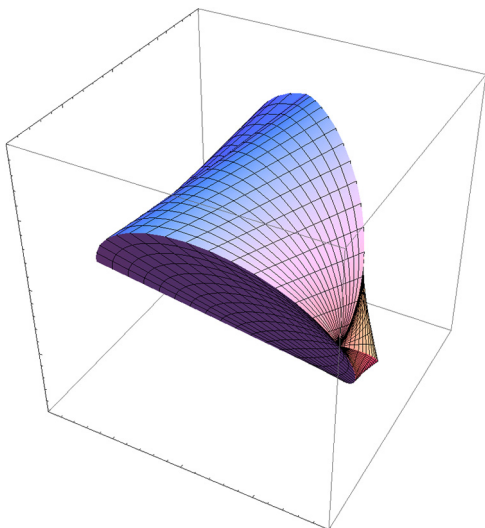


Fig. 5 Region of reconstruction for $-\pi/2 \leq t \leq \pi/2$. For $0 \leq t \leq \pi$, $\pi/2 \leq t \leq 3\pi/2$, or $\pi \leq t \leq 2\pi$, the region of reconstruction is rotated accordingly.

4 Discussions and Conclusion

The issue we have addressed in this paper is quite fundamental. A main question is how one performs scanning so that data acquisition can be done rapidly, continuously, and consecutively in order to monitor changes of an object over time. If we use multiple x-ray sources, how can one make the scanning as independent and symmetric as possible in order to extract the maximum amount of information? Aided by the concept of a tetrahedron, our paper has offered an initial investigation in which consecutive reconstructions can be made in each quarter turn of the rotation. The standard single-source scanning scheme along a spiral trajectory, however, requires a complete rotation cycle to reconstruct the PI-line region inside the object. Compared with this spiral scanning at the same angular rotation speed, our orthogonal-rotation-based tetrahedral scanning can reduce the period of a complete scan by about 75 percent.

To underline future possibilities of CT architectures and suggest practical relevance of our proposed designs, we note that over past years, exciting progress has been made in the x-ray source and detector technologies, which have tremendous implications for CT architectures. In addition to the carbon nano-tube x-ray sources, pyro-electro-mechanical electron sources are also promising.^{5,6} As another example, triboelectric x-ray sources do not require a high voltage supply and produce x-rays by rapidly contacting silicone and a metal-loaded epoxy in a vacuum. With future distributed sources, any scanning trajectories can be electronically steered across x-ray sources densely distributed over a spherical or other surface. As far as detectors are concerned, advanced digital-pixel read-out integrated circuits (ROICs) and flexible electronics are being developed. These have been applied to infra-red and visible imaging, and would be extended for stretchable and reconfigurable x-ray imaging.

Subsequently, we hypothesize that x-ray sources and detectors would be built together, distributed wherever needed around an object to be imaged, and adjusted whenever necessary to accomplish specific tasks. A basic element is neither a source nor a detector, but for functionalities of both of them which can be termed as asourcector (source + detector). Our point is that mechanical scanning is no longer preferred and that electronic scanning will achieve what we have proposed in this paper. Our tetrahedral scanning mode is the perfect mosaic that the four source vertices and the four detector panels enclose an object support seamlessly. For a given field of volume, more source-and-detector pairs will demand a larger system size, while less source-and-detector pairs will under-utilize the available gantry space. Hence, these four source-and-detector pairs are in the most compact and cost-effective combination, and holds a great promise for futuristic imaging applications.

In conclusion, we have proposed the tetrahedron-based scanning mode assuming four pairs of x-ray sources and detectors. These rotations can be implemented by rotating the supporting circumsphere, spinning the object inside the circumsphere, or electronically steering distributed source elements. Our work opens a new direction for x-ray imaging architectures.

Acknowledgments

The authors were partially supported by NIH/NIBIB grant #R01 EB011785 and NSF/MRI grant #0923297.

References

1. A. Katsevich, "Theoretically exact filtered back projection-type inversion algorithm for Spiral CT," *SIAM (Soc. Ind. Appl. Math.) J. Appl. Math.* **62**(6), 2012–2026 (2002).
2. S. S. Orlov, "Theory of three dimensional reconstruction, I conditions for a complete set of projections, II the recovery operator," *Sov. Phys. Crystallogr.* **20**(3), 312–314; **20**(4), 429–433 (1975).
3. J. Zhao et al., "Minimum detection window and inter-helix PI-line with triple-source helical cone-beam scanning," *J. X-Ray Sci. Technol.* **14**(2), 95–107 (2006).
4. P. Y. Lena, Y. Hengyong, and G. Wang, "Determination of exact reconstruction regions in composite-circling cone-beam tomography," *Med. Phys.* **36**(8), 3448–3454 (2009).
5. G. Rosenman et al., "Electron emission from ferroelectrics," *J. Appl. Phys.* **88**(11), 6109–6161 (2000).
6. W. P. Kang et al., "Electron emission from silicon tips coated with sol-gel ($\text{Ba}_{0.67}\text{Sr}_{0.33}$) TiO_3 ferroelectric thin film," *J. Vac. Sci. Technol. B* **19**(3), 1073–1076 (2001).